EM Local Heating with HF Electric Fields

MANOCHEHR KAMYAB HESSARY, MEMBER, IEEE, AND KUN-MU CHEN, FELLOW, IEEE

Abstract—**Capacitor-plate applicators consisting of a pair of flat-plate electrodes, energized by a HF voltage, are utilized to induce heating inside a biological body for the purpose of hyperthermia cancer-therapy. In this paper, a theoretical analysis for such applicators is presented. A pair of coupled integral equations for the unknown total induced electric field inside the body and the charge density on the electrodes is derived and solved numerically for several different cases. The distribution of the specific absorption rate (SAR) of energy inside the body is obtained for each case. The body-electrode coupling is taken into account. A theoretical scheme for synthesizing proper potential distributions on two arrays of subelectrodes for inducing a desirable SAR distribution inside the body is also developed. Using such arrays of subelectrodes, the excessive heating at the fat layer of the body may be avoided. An experiment has been conducted to test the theory.**

I. Introduction

HYPERTHERMIA cancer-therapy has attracted the attention of many medical researchers in recent years. It has been found that, when the temperature of a tumor is raised a few degrees above that of the surrounding tissues, the accompanying chemo- or radio-therapy becomes more effective in treating the tumor. In the combined therapy of malignancies, the objective is to find a noninvasive method by which to heat the tumor without overheating other parts of the body. A nonradiating HF electric field has been found to be a convenient means of inducing heat inside a biological body. This method can be implemented by putting the body between a pair of capacitor-plate electrodes and it has resulted in tumor eradications in tumor-bearing laboratory animals [1], [2] and humans [3].

Even though a parallel-plate applicator has been used with some success, it suffers a major shortcoming—it induces an excessive heating in the fat layer on the body surface. This phenomenon is easily understood because the induced electric field by this applicator at the fat–muscle interface is mainly perpendicular, thus, the electric field in the fat layer with lower permittivity and conductivity is many times higher than that in the muscle layer that has high permittivity and conductivity. Since the specific absorption rate (SAR) of energy is proportional to the square of the electric field and only proportional to the conductivity, the SAR in the fat layer will be much higher than that in the muscle layer. This shortcoming can be over come if, instead of using two electrodes with two constant potentials, two arrays of subelectrodes with proper potential distributions are designed in such a way that the arrays maintain a minimum electric field (or SAR) at the fat layer and a maximum electric field at the internal tumor region. The design procedure for such arrays of subelectrodes is presented in this paper.

In the first part of this paper, the interaction between a pair of energized parallel-plate electrodes and a biological body placed between the two electrodes is studied theoretically. The coupling between the electrodes and the body is taken into account. This body-electrode coupling has been neglected, for simplicity, in our previous studies [4]–[6]. A pair of simultaneous integral equations for the total electric field inside the body and the charge density on the electrodes is developed and solved numerically with a computer. The distributions of SAR and the electric field inside the body are calculated for a variety of cases. In the second part of this paper, a theoretical scheme is developed for inducing a desirable SAR distribution inside the body with two arrays of subelectrodes with proper potential distributions. A numerical example is given to demonstrate such arrays of subelectrodes which induce a maximum SAR in the internal muscle region while maintaining a minimum SAR at the fat layer. The last part of this paper discusses an experimental study which was conducted to verify the accuracy of the theoretical results of this paper.

II. Theoretical Analysis

Consider the situation as shown in Fig. 1, where a biological body of conductivity $\sigma(\vec{r})$, permittivity $\epsilon(\vec{r})$, and permeability μ_0 is placed between two electrodes. A potential difference V with a time variation factor $e^{j\omega t}$ is maintained between the electrodes. At any point inside the body, the total EM field is the sum of incident and scattered fields, i.e.

$$\vec{E}(\vec{r}) = \vec{E}^i(\vec{r}) + \vec{E}^s(\vec{r}) \tag{1}$$

$$\vec{H}(\vec{r}) = \vec{H}^i(\vec{r}) + \vec{H}^s(\vec{r}) \tag{2}$$

where $\vec{E}^i$, $\vec{H}^i$ are the incident EM fields maintained by the charge and current on the electrodes, and $\vec{E}^s$, $\vec{H}^s$ represent the scattered EM fields maintained by the induced current and charge in the body.

It has been shown [7] that the scattered EM fields satisfy the following Maxwell's equations:

$$\nabla X\vec{E}^s(\vec{r}) = -j\omega\mu_0\vec{H}^s(\vec{r}) \tag{3}$$

$$\nabla X\vec{H}^s(\vec{r}) = \vec{J}_{eq}(\vec{r}) + j\omega\epsilon_0\vec{E}^s(\vec{r}) \tag{4}$$

where $\vec{J}_{eq}(\vec{r}) = \tau(\vec{r})\vec{E}(\vec{r})$ is the equivalent current density and $\tau(\vec{r}) = \sigma(\vec{r}) + j\omega(\epsilon(\vec{r}) - \epsilon_0)$ is defined as the complex conductivity of the body. The solution to scattered electric

Manuscript received November 15, 1982; revised January 23, 1984. This research was supported by NSF under Grant No. ECS-8001772.

The authors are with the Department of Electrical Engineering and Systems Science, Michigan State University, East Lansing, MI 48824.

0018-9480/84/0600-0569$01.00 ©1984 IEEE

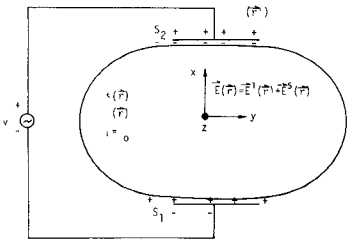

Fig. 1. A pair of electrodes energized by a HF voltage placed across a biological body for local heating.

field $\vec{E}^s$ inside the body can be expressed as [8]

$$\vec{E}^s(\vec{r}) = P\cdot V\cdot \int_{V_{\text{body}}} \vec{J}_{eq}(\vec{r}')\cdot \overleftrightarrow{G}(\vec{r},\vec{r}')\, dv - \frac{\overleftrightarrow{I}\cdot\vec{J}_{eq}(\vec{r})}{3j\omega\epsilon_0} \tag{5}$$

where $\overleftrightarrow{G}(\vec{r},\vec{r}') = -j\omega\mu_0(\overleftrightarrow{I} + \nabla\nabla/k_0^2)G_0(\vec{r},\vec{r}')$ is the tensor Green's function, $\overleftrightarrow{I} = \hat{x}\hat{x} + \hat{y}\hat{y} + \hat{z}\hat{z}$ is the unit dyadic and $G_0(\vec{r},\vec{r}') = e^{-jk_0|\vec{r}-\vec{r}'|}/4\pi|\vec{r}-\vec{r}'|$ and $k_0 = \omega\sqrt{\mu_0\epsilon_0}$. The symbol $P\cdot V\cdot$ stands for the principal value and means that the source point should be excluded by a small limiting sphere while evaluating the integral over the volume of body.

From (1) and (5), we obtain

$$\left(1+\frac{\tau(\vec{r})}{3j\omega\epsilon_0}\right)\vec{E}(\vec{r}) - P\cdot V\cdot\int_{V_{\text{body}}} \tau(\vec{r}')\vec{E}(\vec{r}')\cdot\overleftrightarrow{G}(\vec{r},\vec{r}')\, dv = \vec{E}^i(\vec{r}). \tag{6}$$

The incident electric field $\vec{E}^i(\vec{r})$ is mainly due to the charge deposited on the electrodes and can be expressed as

$$\vec{E}^i(\vec{r}) = \frac{-1}{\epsilon_0}\nabla\int_{\text{electrodes}} \eta_e(\vec{r}'')G_0(\vec{r},\vec{r}'')\, ds \tag{7}$$

where $\eta_e(\vec{r}'')$ is the density of electric charge at point $\vec{r}''$ on the electrodes. In this calculation of the incident electric field $\vec{E}^i$ between the electrodes, the effect due to the currents flowing on the electrodes has been neglected. This approximation is justified in the region between two capacitor-plate electrodes because, on a pair of electrodes, electric charges of large magnitude and opposite signs exist while the currents flow transversely and in opposite directions on this pair of electrodes. Thus, for the maintenance of $\vec{E}^i$ between the electrodes, the contribution due to the current (or the vector potential) is small compared to that due to the charge (or the scalar potential).

With (7), (6) represents an integral equation for the unknown total electric field inside the body and unknown electric charge density on the electrodes. A second integral equation in terms of the charge densities on the electrodes and on the body surface can be written as

$$V_e(\vec{r}_e) = \frac{1}{\epsilon_0}\left[\int_{s_{\text{electrodes}}} \eta_e(\vec{r}')G_0(\vec{r}_e,\vec{r}')\, ds + \int_{s_{\text{body}}} \eta_b(\vec{r}'')G_0(\vec{r}_e,\vec{r}'')\, ds\right] \tag{8}$$

where $V_e(\vec{r}_e)$ is the potential at a point $\vec{r}_e$ on the electrodes and η_b is the density of the charge induced on the surface

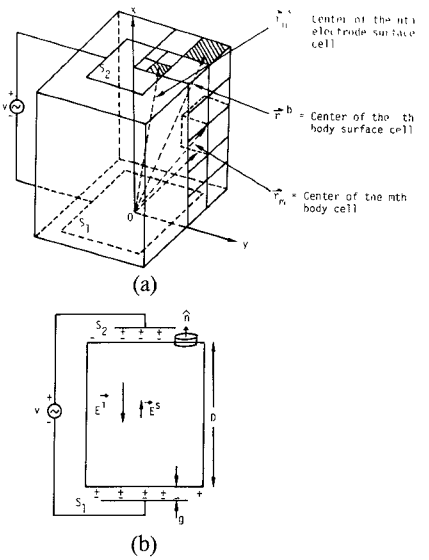

Fig. 2. (a) The geometry of a body placed between two electrodes. (b) The side view of the body and the electrodes.

of body. We have assumed no induced charge inside the body and neglected its effect. For a heterogeneous body, there are charges induced at the interfaces of different tissues. However, these charges are more distant from the electrodes and imbedded in a conducting body, thus, their effects in maintaining the potential on the electrodes will be neglected for simplicity.

Based on the continuity of electric current, it is easy to show that the following relation holds between η_b and the total electric field $\vec{E}$ in the surface layer of the body:

$$\eta_b(\vec{r}) = \frac{\tau(\vec{r})\hat{n}(\vec{r})\cdot\vec{E}(\vec{r})}{j\omega} \tag{9}$$

where $\hat{n}(\vec{r})$ is the outward unit vector normal to the surface body at point $\vec{r}$. Using (9), (8) becomes

$$V_e(\vec{r}_e) = \frac{1}{\epsilon_0}\left[\int_{s_{\text{electrodes}}} \eta_e(\vec{r}')G_0(\vec{r}_e,\vec{r}')\, ds + \frac{1}{j\omega}\int_{s_{\text{body}}} \tau(\vec{r}'')\hat{n}(\vec{r}'')\cdot\vec{E}(\vec{r}'')G_0(\vec{r}_e,\vec{r}'')\, ds\right]. \tag{10}$$

Equation (10) in conjunction with (6) constitutes a pair of coupled integral equations for the unknown total electric field $\vec{E}(\vec{r})$ and the unknown charge density on the electrodes η_e. The well-known moment method [9] is employed to solve these equations numerically. For this purpose, we assume a cubic block of conducting body placed between two square electrodes as shown in Fig. 2. With these arrangements, a four-quadrant symmetry exists in the geometry of the problem; therefore, we need to find the unknowns in one quadrant only. The desired quantities in other quadrants may be obtained easily by utilizing the symmetry.

To apply the moment method, we divide 1/4 of the body volume into N cubic subvolumes; similarly, 1/4 of the electrodes are partitioned into a total number of N' square subareas. It has been shown [7] that point matching of (6) at the center of each body cell leads to the following set of linear algebraic equations for the unknown three components of the electric field at the center of each body cell:

$$(3N)\begin{bmatrix} G_{xx} & G_{xy} & G_{xz} \\ G_{yx} & G_{yy} & G_{yz} \\ G_{zx} & G_{zy} & G_{zz} \end{bmatrix}^{(3N)} \begin{bmatrix} E_x \\ E_y \\ E_z \end{bmatrix} = \begin{bmatrix} E_x^i \\ E_y^i \\ E_z^i \end{bmatrix}. \tag{11}$$

The $[G]$ matrix is a $3N \times 3N$ matrix, while $[E]$ and $[E^i]$ are $3N$ column matrices representing the total electric field and the incident electric field at the centers of N cells. The elements of $[G]$ have been defined in [7]. Based on (7), the column matrix $[E^i]$ can be expressd in terms of the charge densities on the centers of the electrode subareas as

$$(3N)\begin{bmatrix} E_x^i \\ E_y^i \\ E_z^i \end{bmatrix} = \begin{bmatrix} A_x \\ A_y \\ A_z \end{bmatrix}^{(N')} \begin{bmatrix} \eta_e^1 \\ \vdots \\ \eta_e^{N'} \end{bmatrix} \tag{12}$$

where $[A]$ is a $3N \times N'$ matrix and $[\eta_e]$ is an N' column matrix representing the charge densities on the electrode subareas. Combining (11) and (12) gives

$$(3N)\begin{bmatrix} G_{xx} & G_{xy} & G_{xz} & A_x \\ G_{yx} & G_{yy} & G_{yz} & A_y \\ G_{zx} & G_{zy} & G_{zz} & A_z \end{bmatrix}^{\begin{matrix}(3N)\\ \\ \\ (N')\end{matrix}} \begin{bmatrix} E_x \\ E_y \\ E_z \\ \eta_e^1 \\ \vdots \\ \eta_e^{N'} \end{bmatrix} = 0. \tag{13}$$

By a similar technique, (10) may be transformed into a set of simultaneous linear algebraic equations for the charge densities at the centers of electrode subareas and the electric-field components at the centers of those body cells located at the surface of the body. The result is as follows:

$$(N')\begin{bmatrix} C & 0 & 0 & G^s \end{bmatrix}^{(3N+N')} \begin{bmatrix} E_x \\ E_y \\ E_z \\ \eta_e^1 \\ \cdot \\ \cdot \\ \eta_e^{N'} \end{bmatrix} = \begin{bmatrix} V_e^1 \\ \vdots \\ V_e^{N'} \end{bmatrix} \tag{14}$$

where $[V_e]$ is a column matrix with N' elements representing the potentials at the centers of electrode subareas. In the derivation of (14), the effect of induced charges on the lateral surfaces of the body has been neglected. This is justified since the electric field inside the body is mainly in the X-direction (Fig. 2(b)). The elements of the matrices A, C, and G^s are defined elsewhere [10].

Equations (13) and (14) can be combined into the following matrix form:

$$\begin{bmatrix} G_{xx} & G_{xy} & G_{xz} & A_x \\ G_{yx} & G_{yy} & G_{yz} & A_y \\ G_{zx} & G_{zy} & G_{zz} & A_z \\ C & 0 & 0 & G^s \end{bmatrix} \begin{bmatrix} E_x \\ E_y \\ E_z \\ \eta_e^1 \\ \vdots \\ \eta_e^{N'} \end{bmatrix} = \begin{bmatrix} 0 \\ 0 \\ 0 \\ V_e^1 \\ \vdots \\ V_e^{N'} \end{bmatrix}. \tag{15}$$

We can determine V_e's subject to the condition of vanishing of the tangential component of electric field on the surface of electrodes, i.e.

$$\vec{E}_t(r) = -\nabla_t\phi(\vec{r}) - j\omega\vec{A}_t(\vec{r}) = 0 \text{ for } \vec{r} \in S_1 \text{ and } S_2.$$

At low frequencies $\nabla_t\phi(\vec{r}) \gg j\omega\vec{A}_t(\vec{r})$, thus we have

$$\vec{E}_t(\vec{r}) = -\nabla_t\phi(\vec{r}) = 0$$

which implies that the potential on each electrode is constant. Therefore, we may write

$$V_e^1 = V_e^2 = \cdots = V_e^{N_1} = V_{S1}$$

and

$$V_e^{N_1+1} = \cdots = V_e^{N'} = V + V_{S1}$$

where N_1 is the number of partitions on electrode S_1, while there are $N' - N_1$ partitions on S_2. V_{S1} is the potential of S_1 and, as mentioned before, V represents the potential difference maintained between the electrodes and is a known value.

To define V_{S1}, we consider two separate cases:

A. Grounded Potential Case

One electrode is grounded (S_1 for example), thus $V_{S1} = 0$ and (15) becomes

$$(3N+N')\begin{bmatrix} G_{xx} & G_{xy} & G_{xz} & A_x \\ G_{yx} & G_{yy} & G_{yz} & A_y \\ G_{zx} & G_{xy} & G_{zz} & A_z \\ C & 0 & 0 & G^s \end{bmatrix}^{\begin{matrix}(3N)\\ \\ \\ (N')\end{matrix}} \begin{bmatrix} E_x \\ E_y \\ E_z \\ \eta_e^1 \\ \vdots \\ \eta_e^{N'} \end{bmatrix} = V \begin{bmatrix} 0 \\ 0 \\ 0 \\ 0 \\ 1 \end{bmatrix}^{\begin{matrix}(3N)\\ \\ \\ (N_1)\\ (N_2)\end{matrix}} \tag{16}$$

where $N_1 + N_2 = N'$.

B. Floating Potential Case

In this case, the potential of two electrodes are left floating. As one might expect, unlike the previous case, V_{S1} is not known and a slight modification should be made in (16). It is shown [10] that the required system of linear

equations for this case is of the following form:

$$\begin{bmatrix} & (3N+N'+1) & & & & \\ (3N+N'+1) & \begin{array}{|c|c|c|c|c|}\hline G_{xx} & G_{xy} & G_{xz} & A_x & 0 \\ \hline G_{yx} & G_{yy} & G_{yz} & A_y & 0 \\ \hline G_{zx} & G_{zy} & G_{zz} & A_z & 0 \\ \hline C & 0 & 0 & G^s & -1 \\ \hline 0 & 0 & 0 & S_{pe} & 0 \\ \hline \end{array} & & & \end{bmatrix} \begin{bmatrix} E_x \\ E_y \\ E_z \\ \eta_e^1 \\ \vdots \\ \eta_e^{N'} \\ V_{s1} \end{bmatrix}$$

$$= V \begin{bmatrix} 0 \\ 0 \\ 0 \\ 0 \\ 1 \\ 0 \end{bmatrix} \begin{matrix} (3N) \\ (N_1) \\ (N_2) \end{matrix} \tag{17}$$

where S_{pe} is the area of each electrode subarea. The additional equation introduced in the system (17) is obtained on the basis of the fact that the total charges on the electrodes must be zero, i.e.

$$S_{pe} \sum_{\iota=1}^{N'} \eta_e^{\iota} = 0.$$

III. Numerical Results and Discussion

Equations (16) and (17) were solved by the computer for several numerical examples and in each case the distributions of SAR's (heating pattern) and the induced $\vec{E}$ fields inside the body were found. The detailed evaluation of matrix elements of (16) and (17) is available elsewhere [10].

In the first example, we consider a homogeneous body with dimensions of 6 cm×6 cm×3 cm and a conductivity of 0.5 S/m, and a dielectric constant of 80, placed between two electrodes each with dimensions of 4 cm×4 cm. A gap of 2.5 mm is assumed between the electrode and the body surface. The potential difference between the electrodes is assumed to be 2 V at a frequency of 15 MHz. One quarter of the body is divided into 27 volume cells and the distributions of SAR's and the magnitude of the X-component of the $\vec{E}$ field at the center of each cell are shown for both grounded and floating potential cases in Fig. 3 (y and z components of $\vec{E}$ are negligible). From numerical results, it is noted that most of the power is absorbed in that region of the body which is located between the electrodes. It also is found that the SAR distribution inside the body for the grounded potential case is notably different from that for the floating potential case. In the grounded potential case, the magnitude or absorbed power is minimum near the grounded electrode and increases towards the opposite electrode.

In the second example, two electrodes are assumed to be of different sizes as shown in Fig. 4. The lower electrode S_1 has dimensions of 4 cm×4 cm and the upper one 2 cm×

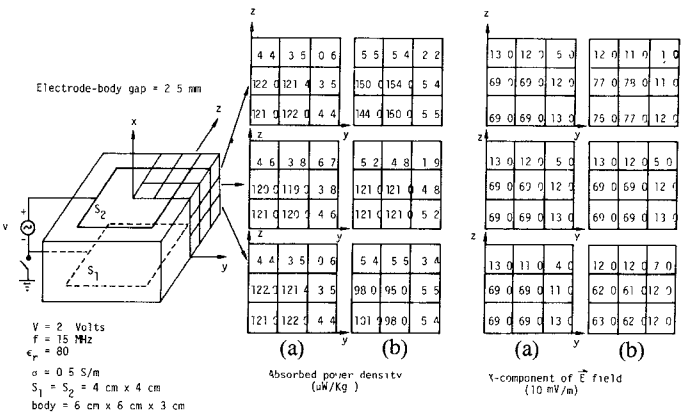

Fig. 3. Distributions of SAR's and the magnitude of the x-component of $\vec{E}$ field at the center of each body cell in 1/4 of a body located between two identical electrodes. (a) Floating potential case. (b) Grounded potential case.

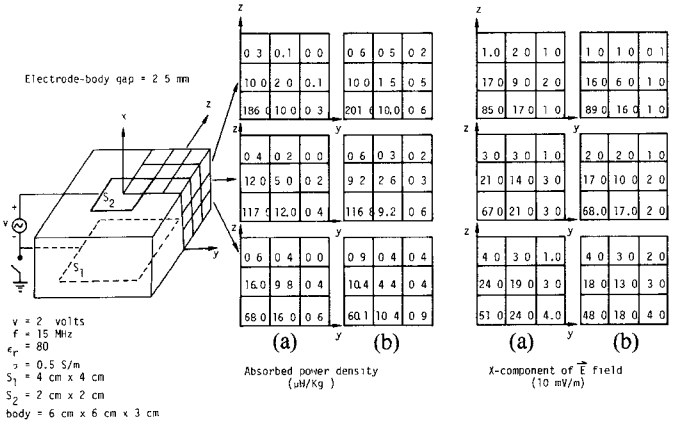

Fig. 4. Distributions of SAR's and the magnitude of the X-component of $\vec{E}$ field at the center of each body cell in 1/4 of a body located between two electrodes of different sizes. (a) Floating potential case. (b) Grounded potential case.

2 cm. The body-electrode gap is again assumed to be 2.5 mm and the body dimensions and parameters are the same as in the preceding example. It is noted that the magnitude of absorbed power is maximum near the smaller upper electrode and decreases rather rapidly toward the larger lower electrode. Grounding S_1 causes the absorbed power density to decrease near the grounded electrode S_1, while it increases near S_2, as shown in Fig. 4(b).

The third example considers a heterogeneous body having a tumor of 2 cm×2 cm×1 cm located at the center of the body (Fig. 5). The conductivity of the tumor is assumed to be slightly different from that of the surrounding tissues, which is 0.5 S/m. The dielectric constant of 80 is assumed for the tumor and the surrounding tissue. The distribution of SAR's for the case when the conductivity of the tumor is 0.35 S/m (0.65 S/m) is shown in Fig. 5(a) and (b). As expected, the magnitude of the absorbed power density increases (decreases) in the tumor with a lower (higher) conductivity than that of the neighboring tissues.

A numerical example is worked out to show how the electric charge is distributed on the electrodes. In this example, two identical electrodes each with dimensions of

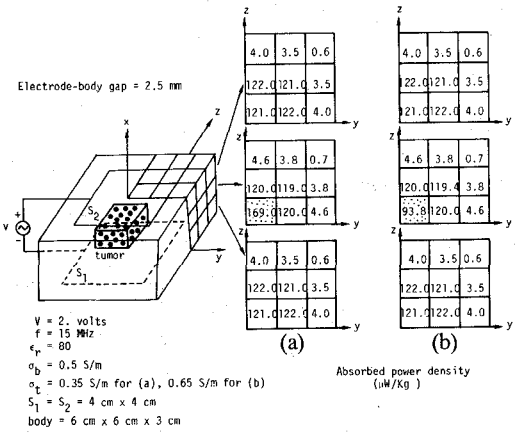

Fig. 5. Distributions of SAR's at the center of each body cell in 1/4 of a heterogeneous body with a tumor at the center located between two electrodes. (a) $\sigma_t = 0.35$ S/m. (b) $\sigma_t = 0.65$ S/m.

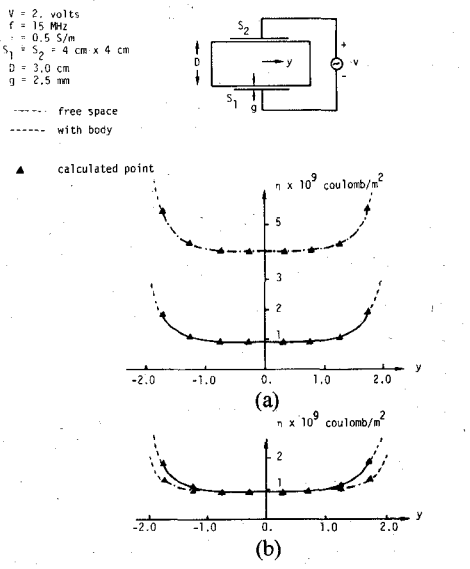

Fig. 6. Distributions of the electric charge along the y axis on the electrode S_2 for the free-space case and the case with a body between the electrodes. In (b), the charge distributions are normalized to show the relative variation.

4 cm×4 cm are placed across a body with dimensions of 6 cm×6 cm×3 cm as shown in Fig. 6. A potential difference of 2 V at 15 MHz is maintained between the electrodes. The distribution of the magnitude of electric charge on the upper electrode (S_2) is shown in Fig. 6 (dashed curves). The distribution of electric charge on the same electrode for the free-space case is also included for comparison. It is noted that the magnitude of electric charge on the electrode in the presence of a body is much higher and is distributed more uniformly as compared to that of the free-space case (solid lines). This phenomenon is depicted in Fig. 6(b), where the distributions of the normalized charge densities for the two cases are compared.

IV. Synthesis of Potential Distributions on Arrays of Subelectrodes for a Desirable SAR Distribution

In the practice of EM local heating with a parallel-plate applicator, the main difficulty to be overcome is to avoid

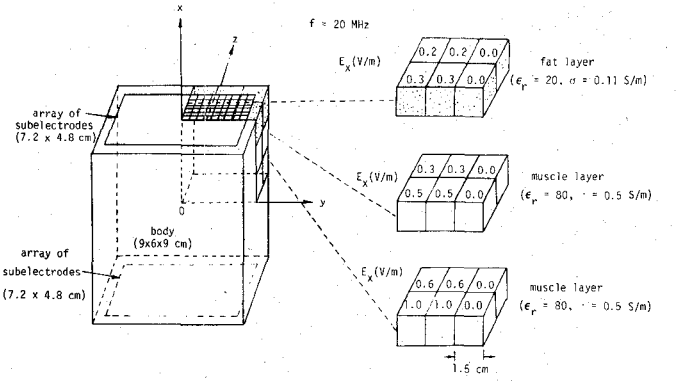

Fig. 7. Desired distribution of the electric field (in the x-direction) in the body to be excited by two arrays of subelectrodes at 20 MHz. The body consists of two fat layers (1.5-cm thickness) and a muscle layer (6-cm thickness). The required potential distributions on the arrays of subelectrodes are shown in Fig. 8.

the excessive heating in the fat layer. This problem can be solved if we divide the two parallel electrodes into two arrays of subelectrodes and then synthesize appropriate potential distributions on the arrays in such a way that a desired SAR distribution in the body is maintained. The desired SAR distribution may have high SAR's in the internal muscle region of the body and low SAR's in the fat layer. The design procedure for such arrays of subelectrodes is explained here.

Assume that a conducting body is placed between two array of N subelectrodes, and the body is divided into a total number of M cubic cells. The components of the total electric field $\vec{E}$ at the centers of the body cells and the charger densities on the subelectrodes are governed by (15). We now assign a desirable distribution of $\vec{E}$ field in the body, and then try to determine the required potentials on the subelectrodes that will maintain the assigned SAR distribution. For example, suppose that we desire to have a distribution of electric fields with only the x-components which has a maximum value at the internal muscle region and a minimum value at the fat layer in the region between the arrays, and a zero field in the region not covered by the arrays, such as that shown in Fig. 7. For this situation, (15) becomes

$$(3M+N)\begin{bmatrix} G_{xs} & G_{xy} & G_{xz} & A_x \\ G_{yx} & G_{yy} & G_{yz} & A_y \\ G_{zx} & G_{zy} & G_{zz} & A_z \\ C & 0 & 0 & G^s \end{bmatrix} \begin{bmatrix} (E_x)_a \\ 0 \\ 0 \\ n_e^1 \\ \vdots \\ \eta_e^N \end{bmatrix} = \begin{bmatrix} 0 \\ \vdots \\ 0 \\ \vdots \\ 0 \\ V_e^1 \\ \vdots \\ V_e^N \end{bmatrix} \quad (3M+N) \tag{18}$$

where $[E_x]_a$ represents the assigned electric fields at the centers of body cells.

In (18), the unknowns are now the charge densities η_e's and the potentials V_e's on the subelectrodes. Thus, (18) represents a set of $3M+N$ equations with $2N$ unknowns

$(\eta_e^1 \dots \eta_e^N, V_e^1 \dots V_e^N)$. To have unique solutions for η_e and V_e, the numbers of equations and unknowns must be the same. That is

$$3M + N = 2N \text{ or } N = 3M.$$

This means that there should be $3M$ subelectrodes in the arrays. With this condition, (18) may be decomposed into the following sets of equations:

$$\begin{bmatrix} A_x \\ \hline A_y \\ \hline A_z \end{bmatrix} \begin{bmatrix} \eta_e^1 \\ \vdots \\ \eta_e^{3M} \end{bmatrix} = - \left[\begin{array}{c|c|c} G_{xx} & G_{xy} & G_{xz} \\ \hline G_{yx} & G_{yy} & G_{yz} \\ \hline G_{zx} & G_{zy} & G_{zz} \end{array}\right] \begin{bmatrix} (E_x)_a \\ \hline 0 \\ \hline 0 \end{bmatrix} \tag{19}$$

and

$$(3M)\left[\begin{array}{c|c|c} (3M) & & \\ C & 0 & 0 \end{array}\right] \begin{bmatrix} (E_x)_a \\ \hline 0 \\ \hline 0 \end{bmatrix} + (3M)[G^s] \begin{bmatrix} \eta_e^1 \\ \vdots \\ \eta_e^{3M} \end{bmatrix} = \begin{bmatrix} V_e^1 \\ \vdots \\ V_e^{3M} \end{bmatrix}. \tag{20}$$

The elements of the matrices $[A]$, $[C]$, $[G]$, and $[G^s]$ can be specified provided that the dimensions of electrodes and body are known. Thus, η_e can be determined from (19). Once η_e is obtained, V_e's can be found by using (20).

As an example, we consider the geometry of Fig. 7, which consists of a body with the dimensions of 9 cm × 6 cm × 6 cm and two arrays of subelectrodes with each array having the dimensions of 7.2 cm × 4.8 cm. The body consists of a muscle layer of 6-cm thickness and two flat layers of 1.5-cm thickness at the top and the bottom. The body is partitioned into 144 1.5-cm cubes ($M = 144$), noting that only one eighth of the partitioned body is depicted due to symmetry. The total number (N) of 432 subelectrodes, each of which has the dimensions of 0.4 cm × 0.4 cm, is then needed in the two arrays. With these arrays of subelectrodes and appropriate potential distributions at 20 MHz, we desire to induce inside the body a distribution of electric fields (having only the x-components) as shown in Fig. 7.

By solving (19) and (20), the distribution of the required potentials (amplitude and phase) on the subelectrodes in a quarter of the upper array is determined to be as that shown in Fig. 8. The required potentials on the subelectrodes of the lower array are the negative of that of the upper array. It is noted that the amplitudes of the required potentials are very high and their signs alternate between many neighboring subelectrodes. This distribution of the required potentials appears to be quite unstable, but it is commonly seen in the field of "super gain" antenna array.

To check the accuracy of this required potential distribution on the subelectrodes, the following numerical test was performed. We used the potential distribution of Fig. 8 but subdivided two cubic body cells (cells 1 and 2 near the center of the body) each into 8 subcells, and recalculated the induced electric fields in these subcells. The results are shown in Fig. 9. The assigned electric field in cell 1 was 1 volt/m in the x-direction, and the recalculated electric fields at the centers of 8 subcells now vary between 1.04 to

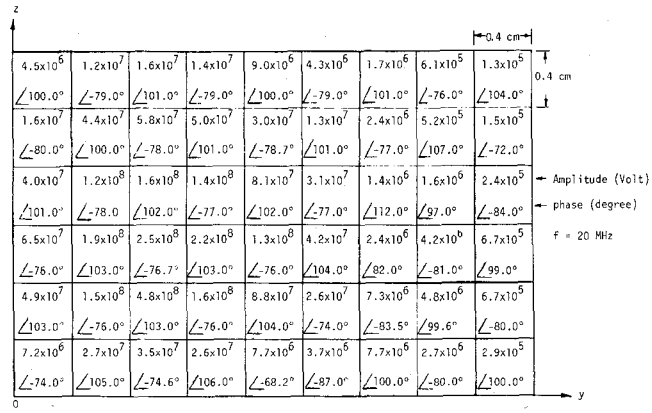

Fig. 8. The required potential distribution on 1/4 of the upper array of subelectrodes that induce a desired distribution of electric fields in the body as shown in Fig. 7.

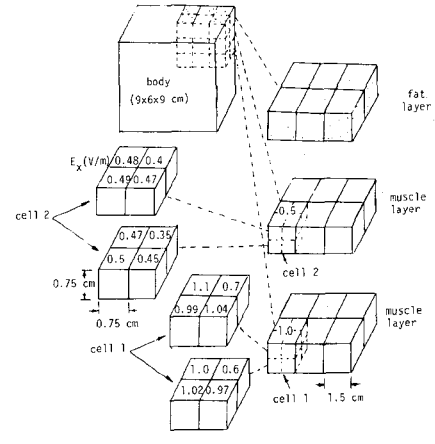

Fig. 9. Numerical test: Cells 1 and 2 are each subdivided into 8 subcells and the induced electric fields at the centers of these subcells are recalculated, based on the potential distributions of Fig. 8 on the arrays of subelectrodes.

0.6 volt/m in the x-direction as shown. The assigned electric field in cell 2 was 0.5 volt/m in the x-direction and the recalculated electric fields at the centers of 8 subcells now range between 0.5 to 0.35 volt/m in the x-direction. This numerical test tends to support the accuracy of the results shown in Fig. 8. It is evident that more accurate results on the required potentials for the subelectrodes can be obtained if the body is subdivided into more cells and the electrodes into more subelectrodes. Unfortunately, with a limited computer storage capacity, we were not able to secure a more accurate solution for the required potential distribution.

The same synthesis procedure can be used to design the arrays of subelectrodes for inducing a more localized SAR distribution. It was found that a higher and more oscillatory potential distribution is usually required to create a more localized SAR distribution in the body.

V. Experimental Results

In order to test the theoretical results found in the preceding sections, a series of experiments was conducted where the magnitude of the total electric field inside a simulated biological body (a plexiglass box containing salt water) was measured by an implantable electric-field probe

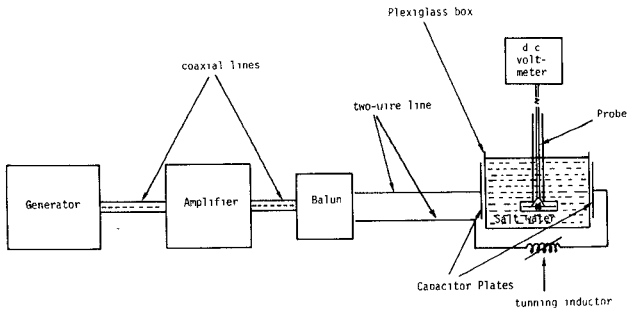

Fig. 10. Experimental setup for the measurement of the electric field in a conducting medium maintained by a pair of capacitor-plate electrodes.

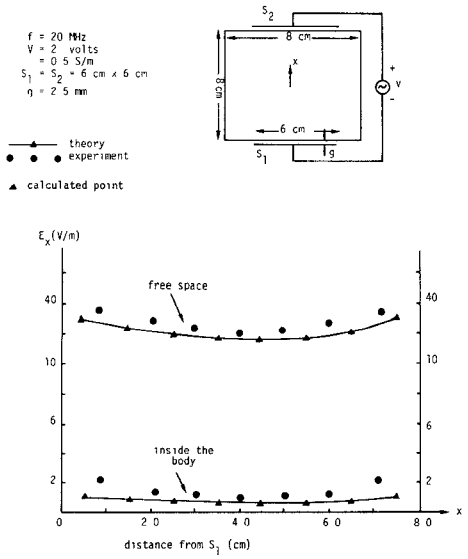

Fig. 11. Distributions of the theoretical and experimental values of the x-component of electric field along the x-axis maintained in the body between two electrodes of equal dimension.

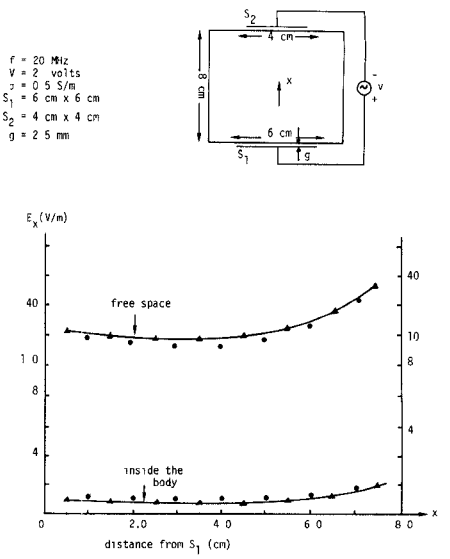

Fig. 12. Distributions of the theoretical and experimental values of the x-component of electric field along the x axis maintained in the body between two electrodes of different dimensions.

developed by our group [11]. The experimental setup is shown in Fig. 10.

In the first experiment, we considered a plexiglass box with dimensions of 8 cm×8 cm×8 cm filled with salt water and two identical 6 cm×6 cm electrodes placed across the box. The measured values of the X-component (dominant component) of $\vec{E}$ field in the central region of solution are shown (discrete points) in comparison with the theoretical values in Fig. 11. The free-space values when no salt water is present are also included in the figure. It is noted that, in the presence of the body, the major part of the voltage is maintained between the body-electrode gaps and, thus, the electric field in the body is much smaller than that of the free-space case. The case of two different size electrodes is considered next. In this case, the upper electrode is 4 cm×4 cm and the lower one is 6 cm×6 cm as shown in Fig. 12. In both cases, the agreement between measured and theoretical values of the X-component of electric field inside the body and in free space in the absence of the body is considered to be good.

VI. Conclusion

In this paper, we present a theoretical method of analyzing the interaction of the EM field maintained between a pair of capacitor-plate electrodes and a biological body located between the electrodes. The coupling between the electrodes and the body has been taken into account. The effects of the geometry of electrodes and the heterogeneity of the body on the induced SAR distribution are studied. A technique of synthesizing proper potential distributions on two arrays of subelectrodes to produce a desirable SAR distribution in a body is also presented. Using such arrays of subelectrodes, the excessive heating at the fat layer may be avoided. Theoretically, it is possible to design two array of subelectrodes with proper potential distributions for inducing a highly concentrated SAR in a localized region inside the body. However, the required potential distributions may become quite unrealistic and unstable. If a less localized SAR distribution is demanded, the required potential distributions become better behaved. In practice, such arrays of subelectrodes may be implemented by a computer-controlled system.

It is noted that the SAR distribution determined in this paper may not represent the actual heating pattern or the temperature distribution. The latter should be determined by considering heat transfer mechanisms that include the blood flow.

References

[1] H. D. Suit and M. Shwayder, "Hyperthermia: Potential as an anti-tumor agent," *Cancer*, vol. 34:1, pp. 122–129, July 1974.

[2] J. E. Robindon, M. J. Wizenberg, and W. A. McCready, "Radiation and hyperthermia response of normal tissue *in situ*," *Radiology*, vol.113:1, pp. 195–198, Oct. 1974.

[3] H. H. Leveen, S. Wapnick, V. Piccone, G. Falk, and N. Ahmed, "Tumor eradication by radiofrequency therapy," *JAMA*, vol. 230, no. 29, pp. 2198–2200, May 17, 1976.

[4] K. M. Chen and B. S. Guru, "Focal hyperthermia as induced by RF radiation of Simulacra with embedded tumors and as induced by EM fields in a model of a human body," *Radio Sci.*, vol. 12, no. 6(S), pp. 27–37, Nov.–Dec. 1977.

[5] B. S. Guru and K. M. Chen, "Hyperthermia by local EM heating and local conductivity change," *IEEE Trans. Biomed. Eng.*, vol. BME-24, no. 5, 473–477, Sept. 1977.

[6] K. M. Chen and S. Rukspollmaung, "Hyperthermia in animal and human bodies induced by EM fields," *J. Bioeng.*, vol. 1, pp. 531–539, 1977.
[7] D. Livesay and K. M. Chen, "Electromagnetic field inside arbitrary shaped biological bodies," *IEEE Trans. Microwave Theory Tech.*, vol. MTT-22, pp. 1273–1280, Dec. 1974.
[8] J. VanBladel, "Some remarks on Green's dyadic for infinite space," *IRE Trans. Antenna Propagat.*, vol. AP-9, pp. 563–566, Nov. 1961.
[9] R. F. Harrington, *Field Computation by Moment Methods*. New York: Macmillan, 1968, ch. 1.
[10] M. K. Hessary, "Local heating of biological bodies with HF electric and magnetic fields," Ph.D. dissertation, Michigan State Univ. East Lansing, 1982.
[11] K. M. Chen, S. Rukspollmaung, and D. P. Nyquist, "Measurement of induced electric field in a phantom model of man," *Radio Sci.*, vol. 17, no. 5(S), pp. 49S-59S, Sept.–Oct. 1982.

✤

Manochehr Kamyab Hessary (M'82) was born in 1947 in Iran. He received B.S. and M.S. degrees, both in physics, from the University of Tehran, Iran, in 1970 and 1976, and Ph.D. in electrical engineering from Michigan State University, East Lansing, in 1982. He returned to Iran in 1983.

Kun-Mu Chen (SM '64–F'76) was born in Taipei, Taiwan, China, on February 3, 1933. He received the B.S.E.E. degree from the National Taiwan University, Taipei, Taiwan, in 1955, and the M.S. and Ph.D. degrees in applied physics from Harvard University, Cambridge, MA, in 1958 and 1960, respectively.

While at Harvard University, he held the C. T. Loo and the Gordon McKay Fellowships. From 1956 to 1957, he was a Teaching Assistant at the National Taiwan University, and from 1959 to 1960 he was a Research Assistant and Teaching Fellow at Harvard University. From 1960 to 1964, he was associated with the Radiation Laboratory, University of Michigan, Ann Arbor, where he was engaged in studies of electromagnetic theory and plasma. In 1962, while on leave from the University of Michigan, he was a Visiting Professor of Electronics at Chao-Tung University, Taiwan. Since 1964, he has been with Michigan State University, East Lansing, first as Associate Professor of Electrical Engineering, and since 1967 as Professor of Electrical Engineering. From 1968 to 1973, he was the Director of the Electrical Engineering program of the Department of Electrical Engineering and Systems Science. He has published numerous papers on electromagnetic radiation and scattering, plasmas, and the interaction of electromagnetic radiation with biological systems.

Dr. Chen is a fellow of the American Association for the Advancement of Science, a member of U.S. Commissions A, B, and C of the International Scientific Radio Union, Sigma Xi, Phi-Kappa-Phi and Tau-Beta-Pi. He is the recipient of the Distinguished Faculty Award from Michigan State University in 1976. He is also the recipient of the Excellent Achievement Award from the Taiwanese American Foundation in 1983.

Microwave Modeling of Rectangular Tunnels

BENJAMIN JACARD AND OSCAR MALDONADO, MEMBER, IEEE

Abstract—**Natural propagation of electromagnetic waves in rectangular tunnels is investigated experimentally at microwave frequencies (1–10 GHz) using a tunnel model of reduced dimensions made of a lossy mixture of sand, water, and salt. The experimental results for the propagation constant of the low-order modes agree satisfactorily with theoretical predictions. Practical applications of the experimental technique are discussed.**

I. Introduction

TO DESIGN IMPROVED communication systems in mine and road tunnels it is necessary to understand the mechanisms of natural propagation. This is not always possible due to difficulties in finding suitable theories for real tunnels. Furthermore, there is not enough experimental data on tunnels to verify the approximate theories proposed. Reliable measurements in real tunnels are difficult and costly due to instrumentation and access problems. For these reasons we propose the use of scale-modeling techniques using tunnel models made from a mixture of sand, water, and salt. This mixture has been previously used for modeling real ground at microwave frequencies [1], [2].

In this paper, experimental results are presented for propagation in a microwave-modeled rectangular tunnel. Results compare satisfactorily with published theory [3], suggesting that this modeling technique could be successfully used for investigating experimentally the propagation in other tunnels of more complex geometry where the theoretical approach would be difficult to apply.

II. Theory of Propagation

An exact analytical solution for propagation in a rectangular tunnel is not possible because of the difficulty in

Manuscript received April 12, 1983; revised January 10, 1984. This work was supported by the University of Chile under Grant DDI 1448-8323.

The authors are with the Department of Electrical Engineering, University of Chile, Santiago, Chile.

0018-9480/84/0600-0576$01.00 ©1984 IEEE